

Microwave Measurements of ^{14}N and D Quadrupole Coupling for (Z)-2-Hydroxypyridine and 2-Pyridone Tautomers

Chakree Tanjaroon, Ranga Subramanian, Chandana Karunatilaka, and Stephen G. Kukolich*

Department of Chemistry, University of Arizona, Tucson 85721

Received: July 9, 2004; In Final Form: August 27, 2004

Rotational spectra for the two tautomers (Z)-2-hydroxypyridine and 2-pyridone and their deuterated isotopomers were measured in the microwave range between 4 and 14 GHz using a pulsed beam Fourier transform microwave spectrometer. Nitrogen and deuterium quadrupole hyperfine structure was completely resolved for many of the observed transitions, and the measured ^{14}N quadrupole coupling tensors are quite different for these two tautomers. The $eQq_{cc}(\text{N})$ values have opposite signs. The ^{14}N quadrupole coupling strengths for (Z)-2-hydroxypyridine in the principal inertial axis system are as follows: $eQq_{aa}(\text{N}) = -0.076(11)$, $eQq_{bb}(\text{N}) = -2.283(6)$, and $eQq_{cc}(\text{N}) = 2.359(6)$ MHz. The ^{14}N and D nuclear quadrupole coupling strengths for (Z)-2-deuteriohydroxypyridine in the principal inertial axis are $eQq_{aa}(\text{N}) = -0.1465(4)$, $eQq_{bb}(\text{N}) = -2.2045(4)$, and $eQq_{cc}(\text{N}) = 2.3510(4)$ MHz and $eQq_{aa}(\text{D}) = -0.0250(9)$, $eQq_{bb}(\text{D}) = 0.1699(4)$, and $eQq_{cc}(\text{D}) = -0.1449(4)$ MHz. The ^{14}N quadrupole coupling strengths for 2-pyridone in the principal inertial axis system are $eQq_{aa}(\text{N}) = 1.496(4)$, $eQq_{bb}(\text{N}) = 1.269(4)$, and $eQq_{cc}(\text{N}) = -2.765(4)$ MHz. The ^{14}N and D nuclear quadrupole coupling strengths for 1-deuterio-2-pyridone in the principal inertial axis system are as follows: $eQq_{aa}(\text{N}) = 1.511(2)$, $eQq_{bb}(\text{N}) = 1.249(5)$, and $eQq_{cc}(\text{N}) = -2.759(5)$ MHz and $eQq_{aa}(\text{D}) = -0.110(7)$, $eQq_{bb}(\text{D}) = 0.354(6)$, and $eQq_{cc}(\text{D}) = -0.244(6)$ MHz. New, improved, experimental rotational constants were obtained for the H and D isotopomers of both tautomers. Kraitchman analysis indicates the “tautomeric” hydrogen atom is at a distance of 2.653(2) Å in 2-hydroxypyridine and a distance of 2.124(1) Å in 2-pyridone from the centers of mass of the two tautomers, respectively. The DFT calculated $eQq(\text{N})$ values for both the tautomers and the deuterated tautomers are in good agreement with the present experimental values. The Townes–Dailey model has been used to analyze the new quadrupole coupling data of the tautomers and the results are presented in terms of nitrogen atom p-orbital occupation numbers.

I. Introduction

The chemistry of keto–enol tautomers has been a subject of considerable interest in organic chemistry for many years, but there is recent interest in these tautomers because they form a hydrogen-bonded dimer, which may provide a simple model for DNA base pair interactions. Extensive, high-resolution electronic spectroscopy studies on these dimers in the gas phase^{1–3} have been reported recently. These recent measurements on the (Z)-2-hydroxypyridine (2hpy) and 2-pyridone (2pyd) dimers have provided new data and increased the motivation to learn more about the spectroscopic properties of these tautomers. The individual tautomers (monomers) are shown in Figure 1. Gas-phase electronic spectroscopy^{4,5} measurements on these monomers was reported earlier. The individual keto–enol tautomers, 2hpy and 2pyd, in recent years have also been studied using X-ray diffraction methods.^{6–8} The structural and equilibrium properties of the keto–enol tautomerism of 2-hydroxypyridine (enol) and 2 pyridone (keto) had been extensively studied earlier. Also, the existence of two tautomers in the solid, liquid, and gas phases were confirmed by various experiments.^{9–13}

Previous microwave spectroscopy¹⁴ measurements have provided some information on the gas-phase structures, equilibrium concentration, dipole moments, and ^{14}N quadrupole coupling strengths for these two tautomers. The ^{14}N quadrupole hyperfine structure for these tautomers, particularly 2pyd, was

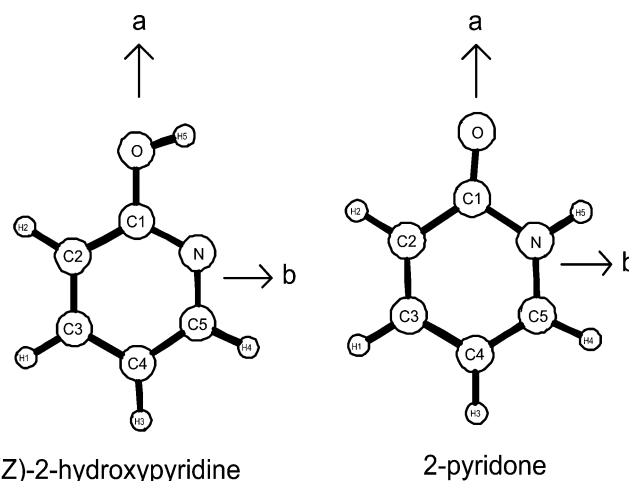


Figure 1. Structures of (Z)-2-hydroxypyridine and 2-pyridone tautomers with their inertial axes labeled.

not well resolved in the previous microwave experiments. This was, in part, due to measurements on high- J transitions. Accurate measurements of quadrupole coupling strengths in this system are important because these strengths provide direct information about electric field gradients and the electronic structure of these molecules, and significant differences in the electronic structure and bonding are revealed by quite different values for the ^{14}N quadrupole coupling.

* To whom correspondence should be addressed. E-mail: kukolich@u.arizona.edu.

TABLE 1: Measured Hyperfine Transitions for (Z)-2-hydroxypyridine and (Z)-2-Deuteriohydroxypyridine, with Fit Residuals^a

a. (Z)-2-Hydroxypyridine ^b												
<i>J</i>	<i>K_a</i>	<i>K_c</i>	<i>F</i>	→	<i>J'</i>	<i>K'_a</i>	<i>K'_c</i>	<i>F'</i>	obsd	obsd – calcd		
0	0	0	1		1	0	1	1	4643.6609(42)	−0.0146		
0	0	0	1		1	0	1	2	4643.7082(22)	0.0097		
1	1	1	2		2	0	2	3	6061.8081(77)	0.0009		
0	0	0	1		1	1	1	1	7700.5475(22)	0.0000		
0	0	0	1		1	1	1	2	7701.2308(26)	−0.0014		
0	0	0	1		1	1	1	0	7702.2619(28)	0.0022		
1	1	1	2		2	1	2	2	8395.3126(48)	−0.0034		
1	1	1	0		2	1	2	1	8395.4615(129)	−0.0067		
1	1	1	1		2	1	2	2	8396.0075(29)	0.0065		
1	1	1	2		2	1	2	3	8396.0706(30)	−0.0037		
1	1	1	1		2	1	2	1	8397.1802(46)	−0.0003		
1	0	1	1		2	0	2	2	9119.1619(101)	0.0073		
1	0	1	2		2	0	2	3	9119.3473(79)	0.0063		
1	1	0	1		2	1	1	1	10177.6001(63)	0.0020		
1	1	0	2		2	1	1	3	10178.7124(91)	−0.0009		
1	1	0	2		2	1	1	2	10179.4444(82)	−0.0027		
2	1	2	3		3	0	3	4	10960.6113(96)	−0.0028		
2	1	2	2		3	0	3	3	10960.9121(49)	0.0053		
1	0	1	1		2	1	2	2	11452.8798(46)	0.0070		
1	0	1	2		2	1	2	3	11453.6029(53)	−0.0053		
2	0	2	2		3	0	3	3	13294.6233(107)	−0.0017		
2	2	1	3		3	2	2	4	13931.0853(48)	−0.0038		
b. (Z)-2-Deuteriohydroxypyridine ^c												
<i>J</i>	<i>K_a</i>	<i>K_c</i>	<i>F₁</i>	<i>F</i>	→	<i>J'</i>	<i>K'_a</i>	<i>K'_c</i>	<i>F'₁</i>	<i>F'</i>	obsd	obsd – calcd
3	1	2	2	3		3	0	3	2	3	6685.6949(9)	−0.0103
3	1	2	4	4		3	0	3	4	4	6686.0301(10)	−0.0019
3	1	2	4	5		3	0	3	4	5	6686.1021(12)	−0.0003
3	1	2	2	3		3	0	3	3	4	6686.3275(2)	0.0019
1	1	1	1	2		0	0	0	1	2	7609.6387(8)	0.0024
1	1	1	2	3		0	0	0	1	2	7610.2905(12)	0.0049
1	1	1	2	2		0	0	0	1	1	7610.3242(4)	−0.0003
2	1	2	2	3		1	1	1	2	3	8159.6764(5)	0.0098
2	1	2	1	2		1	1	1	0	1	8159.8418(7)	−0.0005
2	1	2	3	4		1	1	1	2	3	8160.4173(9)	0.0001
2	0	2	2	3		1	0	1	1	2	8855.6374(5)	0.0023
2	0	2	3	4		1	0	1	2	3	8855.8036(13)	−0.0028
2	1	1	1	2		1	1	0	1	2	9850.8223(5)	0.0063
2	1	1	2	3		1	1	0	1	2	9851.9283(7)	0.0074
2	1	1	2	3		1	1	0	2	3	9852.6172(6)	0.0013
3	1	3	3	4		2	1	2	3	4	12152.8066(7)	−0.0106
3	1	3	3	3		2	1	2	2	2	12153.5859(5)	0.0035
3	1	3	4	5		2	1	2	3	4	12153.6523(4)	−0.0073
3	0	3	3	4		2	0	2	2	3	12936.4941(4)	−0.0057
3	0	3	4	5		2	0	2	3	4	12936.7422(7)	0.0018

^a Frequencies are given in MHz. Experimental measurement errors are in parentheses. ^b The standard deviation of the fit is $\sigma(\text{fit}) = 0.0055$ MHz. ^c The standard deviation of the fit is $\sigma(\text{fit}) = 0.0053$ MHz.

In the present study, we have obtained precise measurements of ¹⁴N quadrupole coupling strengths for 2hpy and 2pyd, and for the monodeuterated isotopomers, (Z)-2-deuterio-hydroxypyridine (2Dpy) and 1-deuterio-2-pyridone (1Dpd). The hyperfine splittings observed for low-*J* transitions in the frequency range 4–14 GHz, using a pulsed-beam Fourier transform microwave spectrometer, were mostly quite well resolved, allowing accurate determinations of the quadrupole coupling tensors. The rotational constants were determined and the new values are in excellent agreements with the previous microwave results.¹⁴ The diagonal elements of the ¹⁴N and D nuclear quadrupole coupling tensors in the inertial and molecular frames were obtained in the present work for 2hpy, 2Dpy, 2pyd, and 1Dpd. Using the ¹⁴N quadrupole moment, we also calculated the electron occupation numbers for the nitrogen p-orbitals, the ionic character in σ and π bonds, and the negative charges on the nitrogen atom for the two tautomers and their corresponding isotopomers. A description of the bonding environment around

the ¹⁴N nuclei was deduced from the quadrupole coupling values and is one of the key findings reported in this paper. These details about the bonding environment may play a significant role in describing the base-pair interaction. Density functional theory (DFT) calculations were performed to calculate the ¹⁴N electric field gradients and quadrupole coupling strengths for these tautomers and for the similar molecules pyrrole and pyridine.

II. Experimental Method

The compound (Z)-2-hydroxypyridine (2hpy) was purchased from Aldrich Chemicals (H5680–0, 97% purity) and used without further purification. The deuterated compounds were synthesized by adding an excess of D₂O to 2hpy and stirring for 5 h. Then the excess D₂O was removed by vacuum. The synthesis was done using a nitrogen atmosphere. The compound was loaded into a glass sample cell inside a drybox in order to

TABLE 2: Measured Hyperfine Transitions for 2-Pyridone and 1-Deuterio-2-pyridone, with Fit Residuals^a

a. 2-Pyridone^b

<i>J</i>	<i>K_a</i>	<i>K_c</i>	<i>F</i>	→	<i>J'</i>	<i>K'_a</i>	<i>K'_c</i>	<i>F'</i>	obsd	obsd – calcd
0	0	0	1		1	0	1	0	4661.5423(22)	0.0015
0	0	0	1		1	0	1	2	4662.2167(27)	0.0026
0	0	0	1		1	0	1	1	4662.6644(29)	0.0014
1	1	1	2		2	0	2	3	6283.3852(87)	0.0007
1	1	1	1		2	0	2	2	6283.6474(75)	0.0002
0	0	0	1		1	1	1	0	7511.9399(28)	-0.0034
0	0	0	1		1	1	1	2	7512.5152(59)	0.0006
0	0	0	1		1	1	1	1	7512.8964(59)	0.0011
1	1	1	1		2	1	2	1	8398.9193(44)	-0.0008
1	1	1	2		2	1	2	3	8399.8011(44)	0.0064
1	1	1	0		2	1	2	1	8399.8631(57)	-0.0089
1	1	1	1		2	1	2	2	8400.3071(17)	0.0042
1	1	1	2		2	1	2	2	8400.6859(37)	0.0023
1	0	1	1		2	0	2	1	9132.8829(59)	0.0042
1	0	1	2		2	0	2	3	9133.6906(88)	0.0056
1	0	1	1		2	0	2	2	9133.8762(124)	-0.0032
1	0	1	0		2	0	2	1	9134.0097(33)	0.0089
1	0	1	2		2	0	2	2	9134.3298(40)	0.0014
1	1	0	0		2	1	1	1	10248.1650(63)	0.0035
1	1	0	2		2	1	1	2	10248.7666(36)	-0.0045
1	1	0	2		2	1	1	3	10249.1788(60)	-0.0003
1	1	0	1		2	1	1	2	10249.5957(93)	-0.0051
1	1	0	1		2	1	1	1	10250.2356(43)	0.0000
2	1	2	3		3	0	3	4	11155.2746(70)	-0.0028
1	0	1	2		2	1	2	3	11250.0948(33)	-0.0003
2	1	2	3		3	1	3	4	12490.7033(55)	-0.0015
2	1	2	2		3	1	3	3	12490.9023(100)	0.0000

b. 1-Deuterio-2-pyridone^c

<i>J</i>	<i>K_a</i>	<i>K_c</i>	<i>F₁</i>	<i>F</i>	→	<i>J'</i>	<i>K'_a</i>	<i>K'_c</i>	<i>F'₁</i>	<i>F'</i>	obsd	obsd – calcd
1	1	1	1	2		2	1	2	1	2	8296.7250(8)	-0.003
1	1	1	2	3		2	1	2	3	4	8297.6192(5)	0.002
1	1	1	1	2		2	1	2	2	3	8298.1083(7)	0.002
1	1	1	1	1		2	1	2	2	2	8298.1842(7)	0.003
1	1	1	2	3		2	1	2	2	3	8298.5125(9)	-0.002
1	0	1	1	2		2	0	2	1	2	9029.4063(9)	0.004
1	0	1	2	2		2	0	2	3	3	9030.2300(15)	-0.005
1	0	1	1	2		2	0	2	2	3	9030.4273(19)	-0.001
1	0	1	2	3		2	0	2	2	3	9030.8880(10)	0.015
1	1	0	0	1		2	1	1	3	2	10185.5820(1)	0.001
1	1	0	0	1		2	1	1	1	2	10185.7578(12)	0.006
1	1	0	2	3		2	1	1	3	4	10186.7677(10)	-0.006
1	1	0	1	1		2	1	1	2	2	10187.1084(4)	-0.001
1	1	0	1	2		2	1	1	2	3	10187.1977(2)	-0.005
2	1	2	3	4		3	0	3	4	5	11179.0801(9)	0.000
2	1	2	1	2		3	0	3	2	3	11179.2476(6)	0.000
2	1	2	3	3		3	1	3	4	4	12326.1182(6)	-0.004
2	1	2	2	3		3	1	3	3	4	12326.3164(11)	-0.004

^a Frequencies are given in MHz. Experimental measurement errors are in parentheses. ^b The standard deviation for the fit is $\sigma(\text{fit}) = 0.0040$ MHz. ^c The standard deviation for the fit is $\sigma(\text{fit}) = 0.0046$ MHz.

minimize the moisture content. The loaded sample cell, which was sealed tightly with removable caps, was inserted into the back of a pulsed valve gas inlet, located inside the sample chamber. The sample was heated to 120 °C, and this temperature was maintained throughout the experiment. We found that it was not necessary to heat the sample to 180–200 °C as had been done in earlier optical and microwave work. It appears that significant decomposition of sample occurs at these higher temperatures. Dark, sticky brown residues could be seen collecting on the inside surface of the sample cell when the sample was heated to 180–200 °C. Neon was used as a carrier gas with the backing pressure maintained at about 0.7 atm.

Both of the samples were pulsed into the microwave cavity at the rate of about 2 Hz. Adjustments in the cavity mode, time delay, attenuator, and power were made to optimize the observed

FID, *S/N* ratio. The molecular signal from the spectrometer cavity was passed through a liquid-nitrogen cooled, MITEQ low-noise amplifier. This amplifier significantly improves the spectrometer *S/N* ratio. Many of the observed FID signals could be seen with a 6:1 *S/N* using single beam pulse.

III. Results

The transition frequencies for the tautomers were measured in the 4–14 GHz range using a pulsed-beam Fourier transform microwave spectrometer,¹⁵ similar to the original Flygare–Balle system.¹⁶ Scanning for molecular signals was straightforward because rotational constants for the two tautomers were known from the previous microwave measurements. Both the a- and b-type dipole transitions were observed for all four compounds,

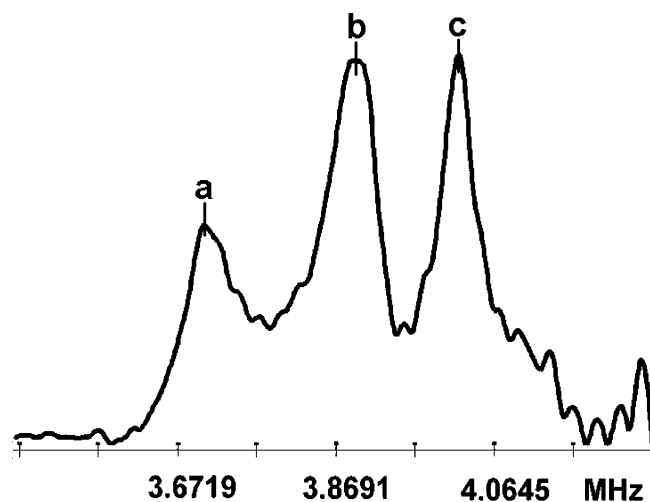


Figure 2. Experimental spectrum for the 2-pyridone $1_{01} \rightarrow 2_{02}$ transitions, showing the ^{14}N quadrupole hyperfine splittings. These three hyperfine structure components have been marked a, b, and c which correspond to hyperfine transitions, $F' \leftarrow F = 3 \leftarrow 2$, $2 \leftarrow 1$, and $1 \leftarrow 0$ respectively (see Table 2a).

with the a-type dipole transitions being stronger. Overall, a total of 22 hyperfine transitions were obtained for 2hpy, 27 hyperfine transitions were obtained for 2pyd and 19 each for the two deuterated tautomers. The observed transition frequencies for 2hpy, 2Dpy, 2pyd, and 1Dpd with measurement errors and fit residuals, are given in Table 1, parts a and b, and Table 2, parts a and b, respectively. An example spectrum of 2pyd, showing the nuclear hyperfine structure splitting of the rotational transition into three components (a, b, c) due to the nitrogen quadrupole coupling, is given in Figure 2 to illustrate a typical molecular signal.

The observed transitions for both tautomers were fit with the SPFIT program,¹⁷ using the Watson *A*-reduced (prolate, I_r representation) Hamiltonian with rotational constants (A , B , C)

and hyperfine strengths as adjustable parameters. The following five adjustable parameters were used in the fit: $P_1 = A$, $P_2 = B$, $P_3 = C$, $P_4 = 1.5eQq_{aa}$, and $P_5 = 0.25(eQq_{bb} - eQq_{cc})$ for each molecule. The fit results obtained for the normal and the deuterated tautomers in this work are shown in Table 3, parts a and b. The set of quartic distortion constants were obtained for both tautomers from the previous microwave measurements in 28–40 GHz range.¹⁴ These distortion values are very small, 0.1–0.5 kHz for D_J , D_{JK} , and D_K , and -0.04 kHz for d_1 and -0.01 kHz for d_2 . For the low- J transitions measured in this work, such small distortion constants do not contribute significantly to the overall rotational energies. The centrifugal distortion constants were too small to be determined outside of the statistical error limits. Fits were tried including the previous centrifugal distortion (CD) constants¹⁴ and with CD constants fixed to zero, and the derived rotational constants did not change within the error limits.

The diagonal elements, eQq_{aa} , eQq_{bb} , eQq_{cc} , of the ^{14}N quadrupole coupling tensors were completely determined for 2hpy and 2pyd. The two sets of quadrupole coupling strengths clearly have opposite signs (see Table 3a). This is believed to be due to the difference in orientation of the nitrogen lone pair p-orbital. The sign of eQq for 2pyd is the same as the sign observed for pyrrole, where the nitrogen lone pair p-orbital is known to lie perpendicular to the aromatic ring system. Similar results were obtained in the case of the deuterated tautomers with regard to the signs of the nuclear quadrupole coupling strengths.

IV. Density Functional Theory Calculations

DFT methods with the gradient-corrected functionals were used to optimize the geometry and calculate electric field gradients for 2pyd, 2hpy, pyrrole, and pyridine. Becke's one-parameter and three-parameter hybrid exchange potentials with Perdew–Wang (PW91)^{18,19} and Lee–Yang–Parr (LYP)²⁰ correlation functionals have been shown to produce accurate predictions of structures and energies for a wide variety of small

TABLE 3: Rotational Parameters Obtained from Fitting the Observed Hyperfine Transitions (Tables 1 and 2) Using SPFIT for 2-Hydroxypyridine (Table 1a), 2-Pyridone (Table 2a), 2-Deuteriohydroxypyridine (Table 1b), and 1-Deuterio-2-pyridone (Table 2b)^a

a. 2-Hydroxypyridine and 2-Pyridone				
parameter	(Z)-2-hydroxypyridine ^c	2-pyridone ^c	2-pyridone ¹⁴	(Z)-2-hydroxypyridine ¹⁴
A	5824.9554(27)	5643.7580(18)	5643.7585(15)	5824.9459(44)
B	2767.5319(12)	2793.46893(71)	2793.47174(98)	2767.5307(20)
C	1876.16268(90)	1868.81993(51)	1868.8234(99)	1876.1647(17)
eQq_{aa}	$-0.076(11)$	1.4962(38)		0.4(3)
eQq_{bb}	$-2.2828(64)$	1.2691(40)		$-2.3(3)$
eQq_{cc}	2.3588(64)	$-2.7653(40)$	$-2.8(2)$	1.9 ^d
$\sigma(\text{fit})$	0.0055	0.0040	0.076	0.067
Δ^b (amu-Å ²)	-0.0026	-0.0342	-0.035	-0.003
b. 2-Deuteriohydroxypyridine and 1-deuterio-2-pyridone				
parameter	(Z)-2-deuteriohydroxypyridine ^c	1-deuterio-2-pyridone ^c	1-deuterio-2-pyridone ¹⁴	(Z)-2-deuteriohydroxypyridine ¹⁴
A	5781.54157(6)	5413.8379(7)	5413.8498(44)	5781.4898(44)
B	2674.43661(1)	2782.8362(1)	2782.8321(24)	2674.4450(29)
C	1828.64323(8)	1838.3065(8)	1838.3102(29)	1828.6362(24)
$eQq_{aa}(\text{N})$	$-0.1465(4)$	1.511(2)		
$eQq_{bb}(\text{N})$	$-2.2045(4)$	1.249(5)		
$eQq_{cc}(\text{N})$	2.3510(4)	$-2.759(5)$		
$eQq_{aa}(\text{D})$	$-0.0250(9)$	$-0.110(7)$		
$eQq_{bb}(\text{D})$	0.1699(4)	0.354(6)		
$eQq_{cc}(\text{D})$	$-0.1449(4)$	$-0.244(6)$		
$\sigma(\text{fit})$	0.0052	0.0046	0.104	0.061
Δ^b (amu-Å ²)	-0.011	-0.040	-0.040	-0.010

^a All fit parameter values are given in MHz. Standard errors are 1σ . ^b Inertial defect, $\Delta = I_c - I_a - I_b$ where B (MHz) = 505379.05 (MHz)/ I_b (amu-Å²) conversion formula is used. Frequencies from ref 14 fit with the Watson *s*-reduced Hamiltonian with rotational constants and quartic distortion terms. ^c This work. ^d For $eQq_{cc} = 1.9$ MHz, no error bar was given.

TABLE 4: Comparison of Experimental to Calculated ¹⁴N Quadrupole Coupling Strengths for Pyridone and 2-Hydroxypyridine^a and Experimental to Calculated D Quadrupole Coupling Strengths in 1-Deuterio-2-pyridone and (Z)-2-Deuteriohydroxypyridine^b

a. ¹⁴ N Quadrupole Coupling Strengths				
molecules	<i>eQq_{aa}</i> (N)	<i>eQq_{bb}</i> (N)	<i>eQq_{cc}</i> (N)	source
Experimental				
pyridone	1.496(4)	1.269(4)	-2.765(4)	this work
2-hydroxypyridine	-0.076(1)	-2.283(6)	2.359(6)	this work
pyridone	-	-	-2.8(2)	ref 14
2-hydroxypyridine	0.4(3)	-2.3(3)	1.9	ref 14
1-deuterio-2-pyridone	1.511(2)	1.249(5)	-2.749(5)	this work
(Z)-2-deuteriohydroxypyridine	-0.1465(4)	-2.2045(4)	2.3510(4)	this work
B3LYP/6-31++G(d,p)				
pyridone	1.430	1.275	-2.705	this work
2-hydroxypyridine	0.047	-1.941	1.894	this work
1-deuterio-2-pyridone	1.498	1.335	-2.833	this work
(Z)-2-deuteriohydroxypyridine	0.049	-2.034	1.985	this work
B3LYP/6-311++G(d,p)				
pyridone	1.509	1.321	-2.831	this work
1-deuterio-2-pyridone	1.582	1.384	-2.966	this work
(Z)-2-deuteriohydroxypyridine	-0.0464	-2.321	2.368	this work
B3PW91/6-311++G(d,p)				
pyridone	1.490	1.263	-2.753	this work
2-hydroxypyridine	-0.0374	-2.159	2.196	this work
1-deuterio-2-pyridone	1.555	1.319	-2.874	this work
(Z)-2-deuteriohydroxypyridine	-0.0385	-2.255	2.293	this work
B3PW91/6-311++G(df,pd)				
pyridone	1.397	1.218	-2.615	this work
2-hydroxypyridine	-0.115	-2.185	2.300	this work
1-deuterio-2-pyridone	1.458	1.271	-2.729	this work
(Z)-2-deuteriohydroxypyridine	-0.119	-2.283	2.403	this work
b. D Quadrupole Coupling Strengths				
molecules	<i>eQq_{aa}</i> (D)	<i>eQq_{bb}</i> (D)	<i>eQq_{cc}</i> (D)	source
Experimental				
1-deuterio-2-pyridone	-0.110(7)	0.354(6)	-0.244(6)	this work
(Z)-2-deuteriohydroxypyridine	-0.0250(9)	0.1699(4)	-0.1449(4)	this work
1-deuterio-2-pyridone	-	-	-	ref 14
(Z)-2-deuteriohydroxypyridine	-	-	-	ref 14
B3LYP/6-31++G(d,p)				
1-deuterio-2-pyridone	-0.005	0.151	-0.147	this work
(Z)-2-deuteriohydroxypyridine	-0.075	0.237	-0.162	this work
B3LYP/6-311++G(d,p)				
1-deuterio-2-pyridone	-0.006	0.159	-0.153	this work
(Z)-2-deuteriohydroxypyridine	-0.078	0.246	-0.168	this work
B3PW91/6-311++G(d,p)				
1-deuterio-2-pyridone	-0.006	0.160	-0.154	this work
(Z)-2-deuteriohydroxypyridine	-0.081	0.251	-0.169	this work
B3PW91/6-311++G(df,pd)				
1-deuterio-2-pyridone	-0.007	0.155	-0.148	this work
(Z)-2-deuteriohydroxypyridine	-0.082	0.245	-0.164	this work

^a Calculations were done using $Q(^{14}\text{N}) = 0.01941(2)$.²² All values are reported in MHz and the theoretical values of quadrupole coupling terms (as obtained from Gaussian) were multiplied by -1. Note: all theoretical values of the electric field gradients obtained from calculations had sign opposite to experiments and were multiplied by -1. ^b Calculations were done using $Q(\text{D}) = 0.00286$ barns.²⁸ All values are reported in MHz.

organic molecules. All density functional calculations were performed on an IBM-640 cluster computer (TINTIN) and HP-Compaq-alpha (AURA) at the University of Arizona using the GAUSSIAN 98 and 03 programs.²¹ The following nonlocal Becke's three-parameter hybrid exchange potentials with Perdew-Wang's and Lee-Yang-Parr correlation functionals were used: B3LYP and B3PW91. Sufficiently large basis sets were selected for carbon, nitrogen, and hydrogen atoms, including both polarization and diffuse functions, 6-31++G(d, p), 6-311++G(d, p), and 6-311++G(df, pd).

The molecular structures of 2pyd and 2hpy are shown in Figure 1. The *a*- and *b*-inertial axes lie in the plane of the

molecule. In this study, geometry optimization was performed before calculating the electric field gradients in 2pd, 2hpy, pyrrole, and pyridine. The optimized atomic coordinates for 2pyd and 2hpy, in their standard orientations, were rotated to the principal inertial axis system using a rotation program written in our laboratory. These atomic coordinates for 2pyd and 2hpy, in their principal axis system, were then used to calculate the electric field gradients. Optimization was done using tight convergence criteria without symmetry constraints, using the keywords opt (nosymm, tight) option. The electric field gradients obtained this way however are the same as those obtained by using the opt (symm, tight) option. The results from DFT

TABLE 5: Comparisons of Experimental to Calculated ^{14}N Quadrupole Coupling Strengths in Pyrrole and Pyridine^a

molecules	eQq_{aa}	eQq_{bb}	eQq_{cc}	source
Experimental				
pyrrole	1.45(2)	1.21(2)	-2.66(2)	ref 23
	1.412(3)	1.292(4)	-2.704(2)	refs 24, 25
pyridine	-4.88(4)	1.43(3)	3.45(2)	ref 23
	-4.908(3)	1.434(3)	3.474(3)	refs 26, 27
B3LYP/6-31++G(d,p)				
pyrrole	1.585	1.197	-2.782	this work
pyridine	-4.301	1.536	3.025	this work
B3LYP/6-311++G(d,p)				
pyrrole	1.589	1.295	-2.884	this work
pyridine	-5.038	1.553	3.484	this work
B3PW91/6-311++G(d,p)				
pyrrole	1.545	1.277	-2.821	this work
pyridine	-4.957	1.551	3.406	this work
B3PW91/6-311+G(df,pd)				
pyrrole	1.475	1.197	-2.672	this work
	1.415	1.215	-2.630	ref 22
pyridine	-4.949	1.444	3.505	this work
	-4.908	1.450	3.458	ref 22

^a Calculations were done using $Q(^{14}\text{N}) = 0.01941(2)$.²² All values are reported in MHz. Note: all theoretical values of the electric field gradients obtained from calculations had sign opposite to experiments and were multiplied by -1 .

calculations are compared to the experimental results obtained from microwave spectra (see Tables 4 and 5).

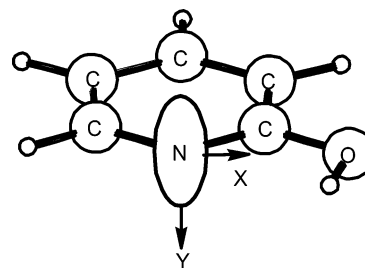
The theoretical ^{14}N quadrupole coupling strengths, eQq_{aa} , eQq_{bb} , and eQq_{cc} , for 2hpy and 2pyd can be determined from the values of electric field gradients q_{aa} , q_{bb} , and q_{cc} , obtained from the DFT calculations. The ^{14}N nuclear quadrupole moment calculated by Bailey²² is $Q(^{14}\text{N}) = 0.01941$ barn. This value of ^{14}N nuclear quadrupole moment obtained by Bailey gives $eQ/h = 4.5617(43)$ MHz/au, and this value can be multiplied by the calculated q_{xx} (au) to give the theoretical ^{14}N quadrupole coupling strengths in MHz. Bailey²² obtained this $Q(^{14}\text{N})$ by carrying out DFT calculations of ^{14}N electric field gradients moment in a number of sp, sp², and sp³ hybridized molecules similar to those discussed in the present paper.

In this work, the calculations of quadrupole coupling strengths from the electric field gradient were obtained using $eQ/h = 4.5617(43)$ MHz/au as reported by Bailey.²² The calculated ^{14}N quadrupole coupling strengths in the inertial axial system for 2pyd and 2hpy were compared to the experimental values obtained from this work. In addition, ^{14}N quadrupole coupling strengths for pyrrole and pyridine were calculated and the results were compared to the previous theoretical and experimental values²³⁻²⁷ (see Table 5).

TABLE 6: Comparison of the ^{14}N Quadrupole Coupling Strengths in the Bond Axis System and p-Orbital Occupation Numbers for Pyridine, 2-Fluoropyridine, 2-Hydroxypyridine, (Z)-2-Deuteriohydroxypyridine, 2-Pyridone, and 1-Deuterio-2-pyridone^a

parameter	pyridine ^b	2-fluoropyridine ^c	2-hydroxypyridine	(Z)-2-deuteriohydroxypyridine	2-pyridone	1-deuterio-2-pyridone
eQq_{xx}	1.43	1.81(5)	1.2612(4)	1.102(1)	1.6335(7)	1.669(1)
eQq_{yy}	3.45	2.82(5)	2.359(6)	2.351(4)	-2.765(4)	-2.759(2)
eQq_{zz}	-4.88	-4.62(5)	-3.620(3)	-3.453(1)	1.1315(6)	1.090(1)
$n_x(p_x)$	1.22	1.20	1.33	1.36	1.37	1.37
$n_y(p_y)$	1.08	1.13	1.26	1.28	1.74	1.74
$n_z(p_z)$	1.71	1.71	1.76	1.77	1.40	1.41
$i_\sigma(\text{NC})$	0.22	0.21	0.33	0.36	$i_\sigma(\text{NC}) = 0.37$	$i_\sigma(\text{NC}) = 0.37$
					$i_\sigma(\text{NH}) = 0.43$	$i_\sigma(\text{NH}) = 0.45$
i_π	0.03	0.13	0.26	0.28	$\pi_c = 0.26$	$\pi_c = 0.26$
C^-	0.52	0.55	0.92	0.99	0.91	0.92

^a The molecules lie in the x-z plane and the y-axis is parallel to the inertial c-axis. Angle for tensor transformation is 31.56 degrees.²⁹ Values for eQq are in MHz. Nitrogen p-orbital populations are n_x , n_y , n_z . The ionic σ and π characters are denoted as i_σ and i_π respectively. Negative charge on nitrogen C^- is in the e unit. ^b All values obtained from ref 23. ^c Nitrogen quadrupole coupling strengths obtained from ref 29.

**Figure 3.** Structure of (Z)-2-hydroxypyridine, showing the bond axis system for the ^{14}N nuclear quadrupole tensor ellipsoid. The molecule is in the x-z plane, with the y axis parallel to the c principal axis of the monomer as discussed in the text.

The same theoretical methods and basis sets were used in the determination of the deuterium (D) electric field gradients. The theoretical values are compared with the experimental results (see Table 4b). The value of $Q(\text{D})$ used is 0.00286 barn and this was obtained using experimental measurements of hyperfine splittings in HD and D_2 by Bishop and Cheung.²⁸ However, the theoretical D quadrupole coupling strengths are not nearly as close to the experimental values, when compared to the ^{14}N results.

V. Nitrogen Quadrupole Coupling and p-Orbital Occupation Numbers

The ^{14}N quadrupole coupling strengths in the bond-axis system and nitrogen p-orbital occupation numbers were obtained for 2hpy, 2Dpy, 2pyd, and 1Dpd, and compared with those for pyridine. The molecular parameters obtained from this analysis are listed in Table 6. The quadrupole coupling strengths along the a, b, and c principal inertial axes of the molecule, are obtained directly from the experimental data. As shown in Figure 3, it is convenient to discuss, and compare, the quadrupole coupling strengths in a bond-axis system where the z-axis lies along the nitrogen lone pair direction, and the plane of the molecule coincides with the x-z plane. The y-axis is perpendicular to the molecular plane and is assumed to lie nearly parallel to the c inertial axis in the case of both the tautomers. For an ortho-substituted pyridine, which has only one plane of symmetry, nitrogen quadrupole coupling is more difficult to determine because the field-gradient perpendicular to the molecular plane axis (y-axis in our orientation) is not defined by symmetry as it is for pyridine. However, the previous study of 2-fluoropyridine²⁹ demonstrated that the quadrupole coupling strengths of ortho-substituted pyridines can be compared to those for pyridine if the coupling tensor a, b, and c axis system values are transformed into the a, b, and c axis system of pyridine.

This transformation is required to bring all the nuclear quadrupole moments into the same basis for comparison.

The transformation from the *a*, *b*, and *c* axis system to the *x*, *y*, and *z* bond axis system of nitrogen, for these molecules requires a rotation of 31.56°. It is not appropriate to use the value of 30° for this transformation, which is the approximate value one obtains for the unsubstituted pyridines. Because of the ortho-substitution for the cases of 2hpy, 2Dpy, 2pyd, and 1Dpd, the principal inertial axis system is reoriented by a slightly greater angle than 30° from the bond-axis system. Hence, the angle of 31.56° was used, which was obtained from a previous study of 2-fluoropyridine,²⁹ even though the true angle will be slightly different for the different isotopomers. The assumption is made that the off-diagonal elements in the *a*, *b*, and *c* principal axis system are negligibly small. This is a required assumption since we did not obtain the off-diagonal quadrupole coupling tensor element, eQq_{ab} , in the inertial axis system in this work. The equations for the transformation to calculate the *x*, *y*, and *z* axis quadrupole tensor components are shown below:

$$eQq_{yy} = eQq_{cc} \quad (1)$$

$$eQq_{zz} = \frac{eQq_{bb} - eQq_{cc} \times \sin^2(\theta)}{\cos^2(\theta) - \sin^2(\theta)} \quad (2)$$

$$eQq_{xx} = -eQq_{cc} - eQq_{zz} \quad (3)$$

The same angle of rotation ($\theta = 31.56^\circ$) is used for all four of the compounds to determine ¹⁴N nuclear quadrupole coupling strengths in the bond axis system even though these angles are slightly different for different molecules. The results obtained using the above transformation are given in Table 6. From this table, it is clear that the ¹⁴N quadrupole coupling strengths for 2hpy, and 2Dpy are similar to those for pyridine and 2-fluoropyridine, suggesting a similar bonding environment around the nitrogen atom. However, the ¹⁴N quadrupole coupling strengths for 2pyd and 1Dpd are quite different, suggesting these have different nitrogen bonding environments. These differences can be related to the fractional number of electrons in the nitrogen-hybridized p-orbitals oriented along the respective *x*, *y*, and *z* axes.

The equations relating the quadrupole coupling strengths and asymmetry parameters to the three-valence p-orbitals of nitrogen are given below. These equations can produce good estimates of the electron occupation numbers for the nitrogen p-orbitals. Detailed discussions of these equations can be found in several standard microwave books and references therein.^{23,30,31}

For a molecule with a nitrogen sp²-hybridized orbital, the equations relating the asymmetry parameter and quadrupole coupling strengths to p-orbital occupation numbers are as follows (with the axis system such that the *y*-axis is perpendicular to the molecular plane):

$$n_x - n_y = \frac{2}{3} \frac{eQq_{xx} - eQq_{yy}}{eQq_{210}} \quad (4)$$

$$eQq_{zz} = \left(\frac{eQq_{210}}{1 + C^- \epsilon} \right) \left[n_z - \frac{1}{2}(n_x + n_y) \right] \quad (5)$$

The electron occupation numbers for p_x, p_y, and p_z orbitals for sp² hybridization are

$$n_x = 1 + i_\sigma \quad (6)$$

$$n_y = 1 + i_\pi \quad (7)$$

$$n_z = 4a_s^2 + (1 + i_\sigma)(1 - 2a_s^2) \quad (8)$$

and for the nitrogen sp³-hybridized orbitals, the following equations can be used (with our axis orientation, the *y*-axis is perpendicular to the molecular plane):

$$\frac{eQq_{yy}}{eQq_{210}} = \frac{(1 - 0.75i_\sigma(\text{NC}) - 0.25i_\sigma(\text{NH}) - \pi_c)}{(1 + 0.3[2i_\sigma(\text{NC}) + i_\sigma(\text{NH}) - \pi_c])} \quad (9)$$

$$eQq_{xx} - eQq_{zz} = \left(\frac{3}{4} \right) (i_\sigma(\text{NC}) - i_\sigma(\text{NH})) eQq_{210} \quad (10)$$

$$i_\sigma(\text{NC}) = a_s^2 = \frac{\cos(\Theta)}{\cos(\Theta) - 1} \quad (11)$$

where a_s^2 is the bonding s-character and Θ is the angle $\angle \text{C1-N-C5}$. The electron occupation numbers for p_x, p_y, and p_z orbital for an sp³-hybridized atom are

$$n_x = 1 + i_\sigma(\text{NC}) \quad (12)$$

$$n_y = 2 - \pi_c \quad (13)$$

$$n_z = 1 + (i_\sigma(\text{NC}) + i_\sigma(\text{NH})) \left(\frac{1}{2} \right) \quad (14)$$

The ionic characters for σ and π bonds are i_σ and i_π , respectively. π_c is the amount of π bonding by the electrons in the p_z orbital. C^- is the negative charge on the nitrogen atom and ϵ is a screening parameter, which is assumed to be 0.30. Using these equations, we calculated the electron occupation numbers for p_x, p_y, and p_z orbitals, the ionic character for σ and π bonds, and the negative charge on the nitrogen atom. The results of this population analysis are given in Table 6.

VI. Discussion

There were no previous measurements of nuclear quadrupole coupling along any axis for the two deuterated tautomers, for either the ¹⁴N or D nuclei. The present study not only gives the ¹⁴N nuclear quadrupole strengths but also gives the D nuclear quadrupole coupling (see Table 3b), thus making this work one of the few studies to obtain the values of D nuclear quadrupole strengths bonded to two different nuclei, namely oxygen (in the case of 2Dpy) and nitrogen (in the case of 1Dpyd). The values of the ¹⁴N nuclear quadrupole coupling strengths, eQq_{aa} , eQq_{bb} , and eQq_{cc} for the D isotopomers are not significantly different (see Table 3, parts a and b) from those for the normal isotopomers. This is not surprising since the electric quadrupole moment of ¹⁴N is small and the rotation angle about the principal axes is small. Even in the case of ³⁵Cl, with an electric quadrupole moment 4 times larger than the ¹⁴N nucleus,³² one observes a small shift of 60 kHz going from CH₃Cl to CH₂DCl for the measured ³⁵Cl nuclear quadrupole coupling strengths.³³ The signs of the ¹⁴N nuclear quadrupole coupling strengths in the deuterated tautomers show the same trend as for the nondeuterated tautomers. The values of nuclear quadrupole coupling strength for D have the same signs for the two tautomers but have different values along the inertial axes (see Table 3b).

A Kraitchman analysis was carried out for the singly substituted isotopomers to determine the coordinates for the OH

TABLE 7: Atomic Coordinates in the Center of Mass (*abc*) System Obtained from the Kraitchman Analysis

	coordinates/Å			
	Z-2-hydroxypyridine ^a	Z-2-hydroxypyridine ^b	2-pyridone ^a	2-pyridone ^b
<i>a</i>	2.52(1)	2.52(8)	0.814(6)	0.82(2)
<i>b</i>	0.833(4)	0.82(3)	1.961(1)	1.95(6)
<i>c</i>	0.0	0.0	0.0	0.0
<i>r</i> _H (com)	2.653(2)		2.124(1)	

^a This work. ^b Reference 14.

hydrogen (in 2hpy) and the NH hydrogen (in 2pyd). The results of these calculations are shown in Table 7 and are in good agreement with the previous study.¹⁴ This analysis determines the distance of the hydrogen atom from the center of mass of the two tautomers (*r*_H(com)). This distance for the case of 2hpy is 2.653(2) Å and that in the case of 2pyd is 2.124(1) Å.

Comparisons of ab initio calculations (DFT), and experimental, quadrupole coupling strengths in the principal inertia axis system suggests that the nitrogen bonding environment and the electric field gradients for 2pyd are similar to those for pyrrole (See Tables 4 and 5). The quadrupole coupling strengths in the inertial axis system for 2hpy are different from the calculated pyridine values. Calculations of *eQq* for 2hpy using B3LYP and B3PW91, with larger basis sets (6-311+G (d, p) and 6-311+G (df, pd)) yielded values (both in magnitude and sign) that agree quite well with the experimental values. It is clear that the larger basis sets, with addition of diffuse and polarization functions, produce better results compared to the results using smaller basis sets. The two sets of quadrupole coupling strengths for the two tautomers are different in magnitude and opposite in sign. For 2hpy, the signs of the ¹⁴N quadrupole coupling strengths (*eQq*_{aa}, *eQq*_{bb}, *eQq*_{cc}) goes as (−, −, +). For 2pyd, the sign of the ¹⁴N quadrupole couplings strengths (*eQq*_{aa}, *eQq*_{bb}, *eQq*_{cc}) goes as (+, +, −). An explanation of the sign reversal observed for 2hpy and 2pyd is discussed below.

The results of high-resolution microwave measurements can now provide a better picture of ¹⁴N quadrupole coupling strengths for 2hpy, 2pyd, 2Dpy, and 1Dpd. With all the three diagonal tensor components in the inertial system determined, we can rotate these inertial components into the bond-axis system of pyridine as discussed in section V. This rotation transformation allows us to obtain the *eQq*_{xx}, *eQq*_{yy}, and *eQq*_{zz} components relative to the pyridine bond axis system. The results of this transformation are shown in Table 6 and the values are compared to the *eQq*_{xx}, *eQq*_{yy}, *eQq*_{zz} components of pyridine²³ and 2-fluoropyridine.²⁹ The ¹⁴N quadrupole coupling strengths for 2hpy and 2Dpy are similar to pyridine and 2-fluoropyridine, whereas the ¹⁴N quadrupole coupling strengths for 2pyd and 1Dpd are markedly different from pyridine and 2-fluoropyridine values. This difference suggests that the 2pyd and 1Dpd nitrogen-bonding environments are different from the 2hpy and 2Dpy bonding environments. The sign reversal observed between 2hpy (*eQq*_{zz} = −3.620(3) MHz) compared to 2pyd (*eQq*_{zz} = 1.1315(6) MHz) suggests that the charge distributions are different in the ring. Because the ring environment is very similar, the orientation of ¹⁴N lone pair electrons alone would affect the way electronic charges distribute along the bond-axis. The previous microwave experiment¹⁴ suggested that 2pyd may contain a pyrrole-type of nitrogen (sp³ hybrid), where the nitrogen lone pair electrons lie perpendicular to the ring system, and that 2hpy contains a pyridine-type of nitrogen (sp² hybridized). Our analysis of the nitrogen p-orbital population (*n*_x, *n*_y, *n*_z) along with σ and π ionic characters (*i* _{σ} and *i* _{π}) for 2hpy and 2pyd provides further evidence supporting this

conclusion. This analysis also indicates that the deuterium substitution does not affect the hybridization, as one might expect.

From Table 6, we can see that *n*_x, the occupation numbers for electrons in the nitrogen p_x orbital (lying in the molecular plane), for the molecules 2hpy, 2Dpy, 2-fluoropyridine, and pyridine are all quite similar, values ranging from 1.2 to 1.33. Good agreement is also seen for the electron occupation numbers *n*_z (also lying in the molecular plane) and *n*_y (perpendicular to the molecular plane) for 2hpy, 2Dpy, 2-fluoropyridine, and pyridine. For these three compounds, the electron occupation number *n*_z is about 1.7, which is significantly larger than the *n*_x and *n*_y occupation numbers. These results show that the nitrogen-bonding environment for 2hpy and 2Dpy is very similar to pyridine and 2-fluoropyridine. The large *n*_z occupation number observed for 2hpy, 2Dpy, pyridine, and 2-fluoropyridine corresponds to placing the nitrogen lone pair electrons in the p_z orbital, which lies in the molecular plane. Thus, the nitrogen-bonding environment obtained for 2hpy and 2Dpy is consistent with sp² hybridization. The occupation numbers, *n*_x, *n*_y, *n*_z, for 2hpy and 2Dpy are slightly larger than the values for 2-fluoropyridine. This larger value in the case of 2-fluoropyridine is possibly due to the difference in the electronegativity between fluorine and oxygen atoms. The higher electronegativity associated with the fluorine atom should decrease electron density in the ring and hence, diminish the negative charge on the nitrogen denoted by C[−]. This explains why C[−] is almost twice as large for the cases of 2hpy and 2Dpy when compared to 2-fluoropyridine.

The nitrogen-bonding environment obtained for 2pyd is consistent with sp³ hybridization. This picture is clear if we examine the electron occupation numbers for 2pyd and compare them to the numbers for 2hpy. The two values of *n*_x and *n*_z for 2hpy and 2pyd are essentially the same in magnitude. For 2pyd, the electron occupation number of the p_y orbital that lies perpendicular to the molecular plane is *n*_y = 1.74. This value of *n*_y is about the same magnitude as *n*_z (which corresponds to the electron occupation number in the p_z orbital that lies along the molecular plane) values of 2hpy, 2-fluoropyridine, and pyridine. We have argued in the previous discussion that the largest occupation number (*n*_z) observed for 2hpy, 2-fluoropyridine, and pyridine must be related to the occupation numbers for the nitrogen lone-pairs electrons. The largest occupation number, *n*_y, for 2pyd suggests that the nitrogen lone-pair occupies the p_y orbital, which lies perpendicular to the molecular plane. This in contrast to 2hpy where for the nitrogen lone pair of electron is in the p_z. Clearly, the signs and magnitudes of ¹⁴N quadrupole coupling strengths for 2hpy and 2pyd give a good indication of where the nitrogen lone-pair electrons are located. We have noted that the deuteration of the two tautomers does not significantly affect the ¹⁴N quadrupole coupling strengths or the occupation numbers for nitrogen lone-pair electrons.

The new rotational constants determined from this work are in excellent agreement with values from the previous microwave measurements (see Table 3a). The experimental inertial defect calculated for 2hpy is $\Delta = -0.0026 \text{ amu-Å}^2$, indicating that this tautomer is a planar molecule. The experimental inertial defect calculated for 2pyd is $\Delta = -0.0342 \text{ amu-Å}^2$. This is about an order of magnitude larger than the value of 2hpy, suggesting a possible slight deviation from planarity, but this could be due only to vibrational averaging effects. A previous fluorescence excitation experiment suggested that the structure of 2pyd is planar in the electronic ground state. However, in a higher electronic excited state, the structure of 2pyd is definitely nonplanar ($\Delta = -1.383 \text{ amu-Å}^2$), as the nitrogen atom in 2pyd is moved out of the molecular plane.⁵

Acknowledgment. We gratefully acknowledge the National Science Foundation for funding support of this research (CHE-0304969). We thank Edward White for his assistance with the drybox. We thank Davian Pedrosa for help in collecting some of the data.

References and Notes

- (1) Roscioli, J. R.; Pratt, D. W.; Smedarchina, Z.; Siebrand, W.; Fernandez-Ramos, A. *J. Chem. Phys.* **2004**, *120*, 11351.
- (2) Borst, D. R.; Roscioli, J. R.; Pratt, D. W.; Florio, G. M.; Zwier, T. S.; Muller, A.; Leutwyler, S. *Chem. Phys.* **2002**, *283*, 341.
- (3) Held, A.; Pratt, D. W. *J. Chem. Phys.* **1992**, *96*, 4869.
- (4) Borst, D. R.; Roscioli, J. R.; Pratt, D. W. *J. Phys. Chem. A* **2002**, *106*, 4022.
- (5) Held, A.; Champagne, B. B.; Pratt, D. W. *J. Chem. Phys.* **1991**, *95*, 8732.
- (6) Penfold, B. *Acta Crystallogr.* **1953**, *6*, 591.
- (7) Wheeler, G. L.; Ammon, H. L. *Acta Crystallogr. Sect. B* **1974**, *B30*, 680.
- (8) Yang, H. W.; Craven, B. M. *Acta Crystallogr.* **1998**, *B54*, 912.
- (9) Albert, A.; Phillips, J. W. *J. Chem. Soc.* **1956**, 1294.
- (10) King, S. S. T.; Dilling, W. L.; Tefertiller, N. B. *Tetrahedron* **1972**, *28*, 5859.
- (11) Beak, P.; Covington, J. B.; Smith, S. G. *J. Am. Chem. Soc.* **1976**, *98*, 8284.
- (12) Beak, P.; Fry, F. S., Jr.; Lee, J.; Steele, F. J. *J. Am. Chem. Soc.* **1976**, *98*, 171.
- (13) Nimlos, M. R.; Kelley, D. F.; Berstein, E. R. *J. Phys. Chem.* **1989**, *93*, 643.
- (14) Hatherley, L. D.; Brown, R. D.; Godfrey, P. D.; Pierlot, A. P.; Caminati, W.; Damiani, D.; Melandri, S.; Favero, L. B. *J. Phys. Chem.* **1993**, *97*, 46–51.
- (15) Bumgarner, R. E.; Kukolich, S. G. *J. Chem. Phys.* **1987**, *86*, 108.
- (16) Balle, T. J.; Flygare, W. H. *Rev. Sci. Instrum.* **1981**, *53*, 33–45.
- (17) Pickett, H. M. *J. Mol. Spectrosc.* **1991**, *148*, 371–377. See also <http://spec.jpl.nasa.gov/ftp/pub/calpgm/spinv.html>.
- (18) Becke, A. D. *Phys. Rev. A* **38** **1988**, 3098.
- (19) Perdew, P. P. *Phys. Rev. B* **33** **1986**, 8822.
- (20) Lee, C.; Yang, W.; Parr, R. *Phys. Rev. B* **37** **1988**, 785.
- (21) Frisch, M. J.; Trucks, G. W.; Schlegel, H. B.; Scuseria, G. E.; Robb, M. A.; Cheeseman, J. R.; Zakrzewski, B. G.; Montgomery, J. A., Jr.; Stratmann, R. E.; Burant, J. C.; Dapprich, S.; Millam, J. M.; Daniels, A. D.; Kudin, K. N.; Strain, M. C.; Farkas, O.; Tomasi, J.; Barone, B.; Cossi, M.; Cammi, R.; Mennucci, B.; Pomelli, C.; Adamo, C.; Clifford, S.; Ochterski, J.; Peterson, G. A.; Ayala, P. Y.; Cui, Q.; Morokuma, K.; Malick, D. K.; Rabuck, A. D.; Raghavachari, K.; Foresman, J. B.; Cioslowski, J.; Ortiz, J. B.; Stefanov, B. B.; Liu, G.; Liashenko, A.; Piskorz, P.; Komaromi, I.; Gomperts, R.; Martin, R. L.; Fox, D. J.; Keith, T.; Al-Laham, M. A.; Peng, C. Y.; Nanayakkara, A.; Gonzalez, C.; Challacombe, M.; Gill, P. M. W.; Johnson, B.; Chen, W.; Wong, M. W.; Andres, J. L.; Gonzalez, C.; Head-Gordon, M.; Replogle, E. S.; Pople, J. A. *Gaussian 98, Revision A.4*, Gaussian, Inc.: Pittsburgh, PA, 1998.
- (22) Bailey, W. C. *Chem. Phys.* **2000**, *252*, 57–66.
- (23) Gordy, W.; Cook, R. L. *Microwave Molecular Spectra*; Chemical Applications of Spectroscopy IX, John Wiley & Son Inc.: New York, 1968 and 1970.
- (24) Bohn, R.; Hillig, K.; Kuczkowski, R. *J. Phys. Chem.* **1989**, *93*, 3456.
- (25) Nygaard, L.; Nielsen, J.; Kircheiner, J.; Maltesen, G.; Rastrup-Anderson, J.; Sorensen, G. *J. Mol. Struct.* **1974**, *22*, 401.
- (26) Heineking, N.; Dreizler, H.; Schwarz, R. Z. *Naturforsch.* **1986**, *41a*, 1210.
- (27) Mata, F.; Quintana, M.; Sorensen, G. *J. Mol. Struct.* **1977**, *42*, 1.
- (28) Bishop, D. M.; Cheung, L. M. *Phys. Rev. A* **1979**, *20*, 381.
- (29) Sharma, S. D.; Doraiswamy, S.; Legell, H.; Mader, H.; Sutter, D. Z. *Naturforsch.* **1971**, *26a*, 1342–1345.
- (30) Townes, C. H.; Schawlow, A. L. *Microwave Spectroscopy*; McGraw-Hill Book Co.: New York **1955**, 243.
- (31) Townes, C. H.; Dailey, B. P. *J. Chem. Phys.* **1949**, *17*, 782.
- (32) Sternheimer, R. N. *Phys. Rev. A* **1972**, *6*, 702.
- (33) Kukolich, S. G.; Nelson, A. C. *J. Am. Chem. Soc.* **1973**, *95*, 680.